P-11
UV CURING OF INORGANIC-ORGANIC HYBRID POLYMERS

VIERA JANČOVIČOVÁ*, PAVOL GEMEINER, and BOHUSLAVA HAVLÍNOVÁ

Department of Printing Arts Technology and Photochemistry IPM, Faculty of Chemical and Food Technology SUT, Radlinského 9, 812 37 Bratislava, Slovak Republic viera.jancovicova@stuba.sk

Introduction

The hybrid (inorganic-organic) polymers are synthetized via the sol-gel process from organoalkoxysilanes, and they have strong covalent or ionic-covalent bonds between the inorganic and organic components. These materials combine the properties of their constituents, such as low processing temperatures, high optical transparency, chemical and thermal stability and hardness. Due to the wide variation in chemical structure that is possible for hybrid polymers, their properties can be adjusted in a wide range[1–4]. Inorganic-organic composite materials (ORMOCER®s: Trademark of the Fraunhofer Gesellschaft zur Förderung der angewandten Forschung e. V., Munich) are well-suited for the specific functionalization of different polymer and paper surfaces. These materials are water-based or dispersed in nontoxic solvents. Curing is performed photochemically or thermally at relatively low temperatures. Resulting layers are transparent, sturdy and chemically stable. The gas permeability of coated papers is significantly reduced and barrier properties to water vapour and odours are enhanced[5,6]. Multilayer, flexible and transparent high-barrier system based on flexible plastic foils, polyethyleneterephthalate (PET) and ethylene-tetrafluoroethylene-copolymer (EFTE) combined with vacuum-deposited, inorganic SiOx layers and hybrid ORMOCER® varnish layer were prepared in different orders on a semiproduction level[7].

Experimental

Materials

ORMOCER® (Fraunhofer Gesellschaft zur Forderung der angewandten Forschung, Munich, Germany), 1-[4-(2-hydroxyethoxy)-phenyl]-2-hydroxy-2-methyl-1-propane-1-one (Irgacure®2959, Ciba, Switzerland), 1-hydroxy-cyclohexyl-phenyl-ketone (Irgacure®184, Ciba, Switzerland), bis(2,4,6-trimethylbenzoyl)-phenylphosphineoxide (Irgacure®819, Ciba, Switzerland) were used.

Preparation of films

The samples were applied immediately after preparation. Various types and amounts of initiator (from 0.5 to 5 wt.%) were added to ORMOCER®, mechanically mixed and stored in opaque bottle. Photocuring reactions were realized on aluminium plates. The defined sample volume (according to layer thickness) was spread on the plate by spin coating and the layer thickness was determined gravimetrically. The layer thicknesses of our samples were 10 μm.

UV curing of coatings

The samples coated on the aluminum plates were irradiated by a medium pressure mercury lamp 250W (RVC, Czech Republic) built into an UV-cure device constructed in our laboratory. The intensity of incident light was changed with the varying distance of the light source from the sample (5 cm = 28 mW cm^{-2}, 12 cm = 12 mW cm^{-2}). The curing process was monitored by ATR-IR spectroscopy (FTIR spectrophotometer EXCALIBUR SERIES Digilab FTS 3000 NX, USA). The degree of conversion of the cured film was determined based on the abosrption of acrylate double bond (twisting vibration at 810 cm^{-1}, stretching vibration at 1630–1640 cm^{-1}) by a baseline method. The degree of conversion X and relative polymerization rate R_p were calculated from well-known equations[8,9]

$$X = 1 - \frac{[A_\lambda]_0}{[A_\lambda]_t} \qquad (1)$$

where $A_{0(\lambda)}$ and $A_{t(\lambda)}$ are the absorbances of monomers C=C bounds measured at chosen wavelength (810 and 1635 cm^{-1}) before and after the exposure to UV light for the time t or exposition dosage, respectively.
The relative polymerization rate R_p was calculated from the equation

$$R_p = (\Delta X/\Delta t) \qquad (2)$$

where X is the conversion degree of monomer's C=C bounds, at the exposure time t. The values of maximum conversion X_{max} and maximum polymerization rate $R_{p,max}$ were obtained from the plots of X and R_p vs. time.

Results

In order to optimize the coating compositions samples of ORMOCER®s containing 0.5, 1, 3 and 5 wt.% of three radical type initiators (Irgacure®184, Irgacure®2595 and Irgacure®819) were prepared. As shown in Fig. 1, during the curing process, a decrease of absorbance can be observed of the bands characteristic for carbon-carbon double bond (810 and 1635 cm^{-1}).

The functional and handling properties of UV cured layers strongly depend on the conversion of the double bond achieved during irradiation. It is obvious that concentration and type of used photoinitiator markedly affects the values of maximum conversion (X_{max}) and maximum rate of polymerisation (Rp_{max}) parameters.

The initial rate of curing at the light intensity 28 mW cm^{-2} for the composition containg Irgacure®184 is the fastest for 5 wt.% content of photoinitiator, where 70 % conversion is achieved within 10 s. The curing of samples with smaller initiator content is slower. However, in the case of all

three samples the curing process was completed and the conversion reached 88–90 % (ref.[5]). At the light intensity 12 mW cm^{-2} (Fig. 2) we observed that the Rp_{max} and X_{max} was reached at the initiator concentration of 1 wt.% (X_{max} 93 %). In the experiment with the increase of the amount of photoinitiator from 1 to 5 wt.%, decreased the double bond conversion as well as the rate of polymerization were observed. The higher concentration of Irgacure®184 probably provides high absorption, and the initiator acts as internal filter.

The results obtained for UV curing of ORMOCER®s with photoinitiator Irgacure®2959 (Fig. 3) at the light intensity 12 mW cm^{-2} are in a good agreement with the results obtained with Irgacure®184.

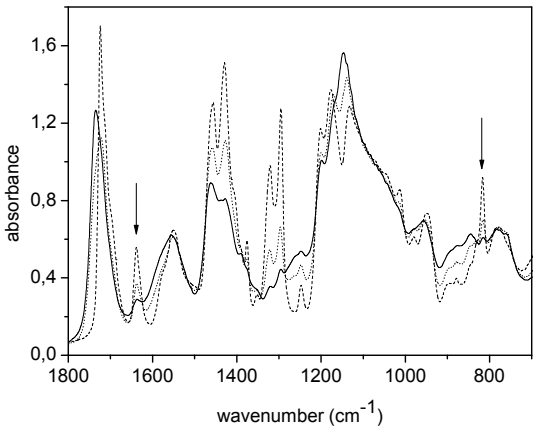

Fig. 1. **Changes in FTIR spectra of ORMOCER®s with 1 % of initiator Irgacure®184 during UV curing** (curing time 0 s – solid line, 70 s – dot line, 900 s – dash line) at the light intensity 12 mW cm^{-2}

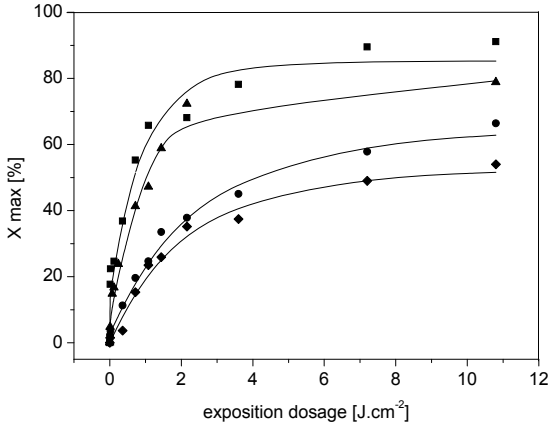

Fig. 2. **Influence of exposition dosage on the UV curing of ORMOCER®s at various Irgacure®184 concentrations** (0.5 % ●, 1 % ■, 2 % ▲ and 5 % ♦; layer thickness 10 μm) at the light intensity 12 mW cm^{-2}

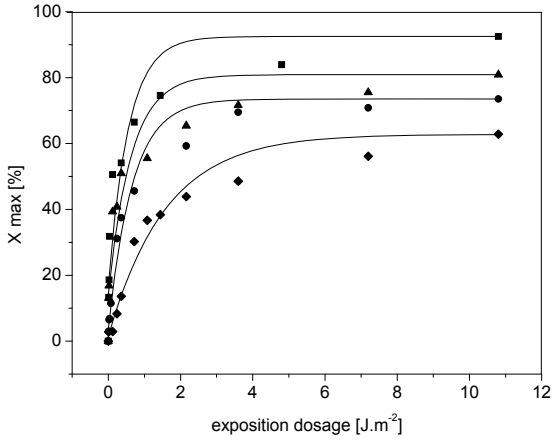

Fig. 3. **Influence of exposition dosage on the UV curing of ORMOCER®s at various Irgacure®2959 concentrations** (0.5 % ●, 1 % ■, 2 % ▲ and 5 % ♦; layer thickness 10 μm) at the light intensity 12 mW cm^{-2}

UV curing of ORMOCER®s was studied also in the presence of the photoinitiator Irgacure®819 at the same light intensity. In this case the photopolymerization didn´t occur effectivelly. Even the high exposition dosage (20 J cm^{-2}) was not enough to cure the coating. The samples were tacky, smelling and cracked. The maximal conversion degrees X_{max} achieved by using each of these three initiators are presented in Fig. 4.

The highest values of X_{max} (around 90 %) were achieved for systems containing Irgacure®184 (1 wt.%) and Irgacure®2959 (1 wt.%). These systems were cured by sunlight (2 hours at noon) and the achieved conversion values were similar for compositions with both initiator (X_{max} 78 % for Irgacure®184 and 72 % for Irgacure®2959). The both composition were sufficiently cured.

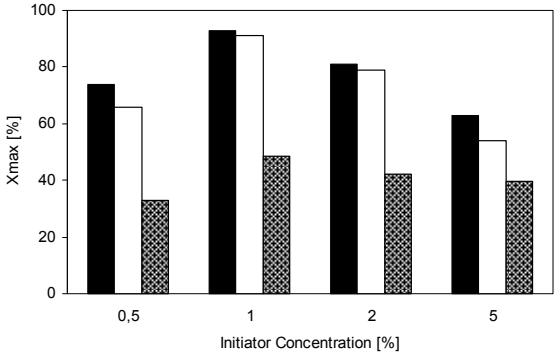

Fig. 4. **The influence of initiator** (Irgacure®184 ■, Irgacure®2595□ and Irgacure®819 ▒) on the maximal degree of conversion at the light intensity 12 mW cm^{-2}

Conclusions

UV curing of compositions containing the hybrid (inorganic-organic) polymers ORMOCER®s and radical photoinitiator type I was monitored by FTIR spectroscopy. The properties of UV cured coatings depend on their compositions (type and concentration of used initiator) as well as on the curing conditions. The highest conversion was achieved for initiators Irgacure®184 and Irgacure®2959 at the initiator concentration 1 wt.%. Both systems were effectivelly cured also by sunlight.

The authors thank the Slovak Grant Agency for the financial support (project VEGA 1/1006/11).

REFERENCES

1. Laskarakis A., Georgiou D., Logothetidis S., Amberg-Schwab S., Weber U.: Mater. Chem. Phys. *115*, 269 (2009).
2. Amberg-Schwab S., Weber U., Burger A., Nique S., Xalter R.: Monatsh. Chem. *137*, 657 (2006).
3. Haas K., Amberg-Schwab S., Rose K., Schottner G.: Surf. Coat. Technol. *111*, 72 (1999).
4. Amberg-Schwab S., Katschorek H., Weber U., Hoffmann M., Burger A.: J. Sol-Gel Sci. Technol. *19*, 125 (2000).
5. Jančovičová V., Amberg-Schwab S., Dzik P., Mikula M.: Chem. Pap. *102*, 1051 (2008).
6. Amberg-Schwab S.: PTS *Symposium Innovative Packaging*, p. C02 Munich (2005).
7. Vaško K., Noller K., Mikula M., Amberg-Schwab S., Weber U.: Central Eur. J. Phys. *7*, 371 (2009).
8. Müller U.: J.M.S.-Pure Appl. Chem. *A33*, 33 (1996).
9. Müller U.: J. Photochem. Photobiol. A: Chem. *239*, 237 (1997).

P-12
PLASMA TREATED THIN TiO_2 SOL-GEL LAYERS ON PLASTIC FOILS

MICHAL ŠANDREJ, MILAN MIKULA*, and PAVOL GEMEINER

Department of Printing Arts Technology and Photochemistry IPM, Faculty of Chemical and Food Technology SUT, Radlinského 9, 812 37 Bratislava, Slovak Republic
milan.mikula@stuba.sk

Abstract

TiO_2 xerogel layers prepared by sol-gel techniques ought to be sintered to more dense, anatase structure, in order to use them in photocatalysis or photovoltaics. Desired sintering temperatures exceed considerably allowable temperature for polymer substrates like PET or PP supposed for printed electronic application. Lower-temperature sintering and reconstruction of xerogel layers could be very beneficial for cheap production of photoactive layers on flexible substrates. Successful sintering of ink-jet printed nano-silver ink by low-pressure plasma was already published. Thin dip coated TiO_2 sol-gel layers (50 nm) deposited on PP, glass and Si-plate were treated in dielectric barrier discharge (DBD) plasma (standard volume and coplanar) in air at atmospheric pressure to study the level of reconstruction of the xerogel layers using FTIR spectroscopy, atomic force microscopy (AFM) and conductivity measurements.

Introduction

Titanium dioxide (TiO_2), well known due to photocatalysis effect, belongs to the most popular materials of present days. It is used in heterogenous catalysis as a photocatalyst, in solar cells for the production of hydrogen and electric energy, as gas sensor, as white pigment, as corrosion protective coating, as an optical coating, in ceramics and in electric devices[1].

With the invention of Dye Sensitized Solar Cell (DSSC) in 1991 (ref.[2]), the new materials get into the interest. Non toxicity, prompt availability and low cost of production process are the most required properties. The synergy of these conditions is found in conventional printing techniques such flexo printing, ofset printing, screen printing and ink-jet, which provides high variability in deposited solutions. The nanostructure layer of TiO_2 is key element in the structure of DSSC and preparation, deposition and modification are frequently investigated.

Preparation of nanostructured TiO_2 layers is based on Sol-Gel method invented around 1880 by investigation of hydrolysis of tetraoxosilicates in acid environment[3]. Sol-gel process is based on chemical reaction of hydrolysis and polycondensation of titania alcoxides, with formation of oxopolymers. These are transformed into oxide network. Condensation continues with gel formation. After evaporation of solution the xerogel is built and the calcination step continues[4,5].

Low-temperature plasma is a technology used for treatment and modifying thin films under low temperature, including inorganic materials. In this technique, nitrogen plasma, oxygen plasma, and argon plasma are typically used reaction sources. Recently, plasma treatments have been used as a calcination step for removal of organic additives and generation of mesoporous films with sol–gel precursors[6].

In this paper attention has been devoted to deposition of thin film TiO_2 layers by dip coating onto PP, glass and Si-plate and additional atmospheric plasma treatment of the xerogel layer. The influence of plasma parameters and exposition time on the layer properties was determined by UV-Vis and FTIR spectral methods and conductivity measurement. The results were compared with results obtained by conventional thermal annealing.

Experimental

Three types of substrates, polypropylene foil (PP, 40 μm, Chemosvit, Slovakia), microscopy slide glass (1.1 mm thick) and Si plate with epitaxial Si layer (111) were coated by 3 % TiO_2 sol, Ti-tetrabuthoxide in waterfree ethanol (stabilized by HNO_3) by simple dip coating (the draw up rate was 10 cm min^{-1}). After 1 day in Lab, the layers prepared on glass and Si substrates were calcinated at different temperatures up

to 400 °C. The layers prepared on PP substrates were treated in atm. pressure plasmas of standard volume DBD (5 kHz, 30 W) and coplanar surface DBD (8 kHz, 300 W) in different exposition times. Afterwards, the layers were characterized by UV-Vis. and FTIR spectroscopy, using diffuse reflectance (CECIL 550) and diamond ATR technique (Excalibur Digi-lab, FTS 3000), respectively. DC and AC conductivities of layers were measured using multimeters Keithley 2000 and Metex M-3650D, and LCR Digibridge Quadtech 1715.

Results

The prepared xerogel layers were free of cracks and precipitates, stable in time and also stable on the flexible PP foil. Plasma treated layers have generally larger scale texture, Fig. 1 (tapping mode AFM, Veeco, CP II).

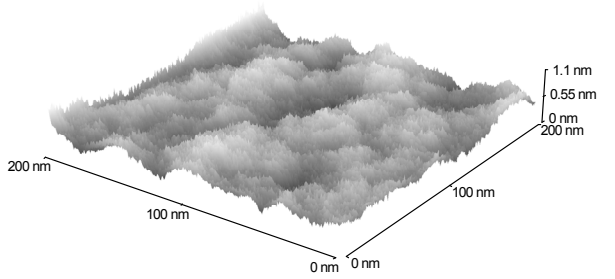

Treated, 10 s, CS DBD

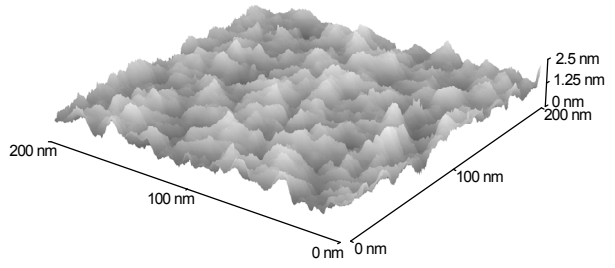

Non-treated

Fig. 1. **Topography of plasma treated and non-treated layers on PP**

Fig. 2. **The xerogel layer on glass with the scratch (50 μm wide) and with the AFM cantilever above the measured edge**

The layer thickness was measured by AFM, scanning the layer scratch on the glass substrate, made by a sharp knife, Fig. 2. The thickness of layers were round 50 nm, while after sintering at 300 °C were reduced to about 35 nm.

UV-Vis. spectra of layers on PP and glass substrates were measured with diffuse reflectance technique to suppress the interference. Al mirror was used as a background also when measured a foil. The layers on Al metalized glass substrates were calcinated up to 400 °C. Some decrease of formal absorbance has occurred mainly for thermal treated samples. The influence of plasma treatment is very small (Fig. 3).

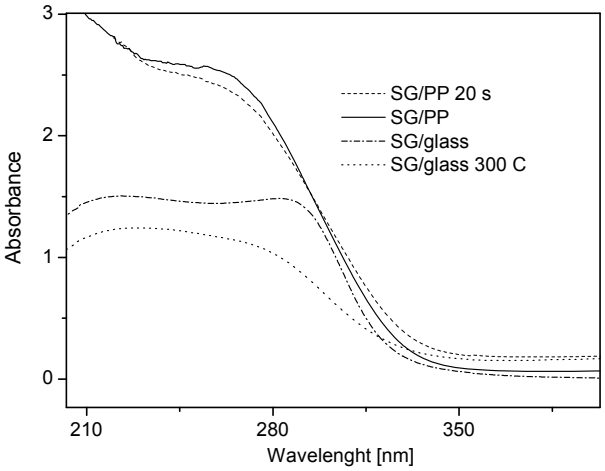

Fig. 3. **Optical density of remission (formal absorbance) in UV spectral region for sol-gel layers on PP (as prepared "SG/PP" and plasma treated 20 s by CSDBD) and on the glass (as prepared "SG/glass" and calcinated at 300 °C**

Measuring FTIR spectra, diamond ATR for glass substrates and (horizontal) HATR techniques for PP substrates were used. However, the difference spectra had to be used because the sol-gel layers were very thin compared with the depth of evanescent wave penetration (Fig. 4).

Conductivity was measured for the layers prepared on Si and Al coated glass substrates, in capacitor like geometry. Most of the samples were not measurable and the rest had a very high dispersion of data. So the error was higher than the mean value itself. However, the evident increase with the plasma treatment, namely for CS DBD was observed.

Conclusions

The dip coated TiO_2 sol-gel layers on PP, glass and Si substrates were plasma treated to achieve reorganization of the xerogel and to increase the electrical conductivity as well. Simultaneously, the xerogel layers on Si and glass substrates were calcinated to find and study the changes in layer structure measuring the FTIR, UV and Vis. spectra and electric conductivity.

Coplanar DBD discharge was more effective than standard volume DBD, regarding conductivity measurements and spectral changes, due to its better discharge homogeneity.

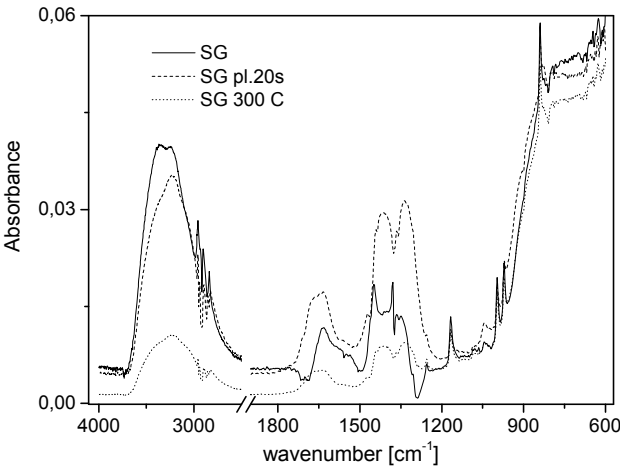

Fig. 4. **Difference FTIR spectra of sol-gel layers on PP (as prepared "SG" and plasma treated 20 s by CSDBD) and on the glass calcinated at 300 °C**

However, the spectral changes with plasma treatment were small comparing with those of thermal treated (that were also small due to very thin layers). Spectral changes have correlated mainly with the water and alcohol removing. The conductivity changes were the most readable, however, the error of measurement was too big and the reproducibility was very pure. If it will enhanced, the electric conductivity would be the most sensitive parameter to structural changes of thin layers, caused by plasma treatment.

The authors thank the Slovak Grant Agency for the financial support (project VEGA 1/1006/11).

REFERENCES

1. Diebold U.: *PhD Thesis*, Department of Physics, Tulane University, 2002.
2. Regan B., Grätzel M., Nature *353*, 737 (1991).
3. Brinker C. J., Scherer G. W.: *The Physics and Chemistry of Sol-Gel Processing, in Sol-Gel Science*, Acad. Press 1990.
4. Suzuki Y., Yoshikawa S.: J. Mater. Res. *19*, 982 (2004).
5. Ruzycki N., Herman G. S., Boatner L. A, Diebold U.: Surf. Sci. Lett. *529*, L239 (2003).
6. Huang J., Ichinose I., Kunitake T., Nakao A.: Langmuir *18*, 9048 (2002).

P-13

DIRECT ADHESION OF RUBBERS TO VARIOUS RESINS DURING CURING USING MOLECULAR ADHESIVES

HIDETOSHI HIRAHARA, KATSUHITO MORI, EIICHI NARITA, YOSHIYUKI OISHI, SUMIO AISAWA, and KUNIO MORI

Graduate School of Engineering, IWATE UNIVERSITY, 4-3-5 Ueda Morioka IWATE, Japan
hiraha@iwate-u.ac.jp

In studying the direct adhesion of rubbers to various resins using molecular adhesives, we investigated 6-triethoxy silyl propylamino-1,3,5-triazine-2,4-dithiols (TES) for the linking of –OH groups on resin surfaces, the TES linking conditions, curing conditions of rubbers, material dependence of the resins, relationship between linked TES concentration and peel strength, and failure behavior. The –OH groups were generated on resin surfaces using an atmosphere corona discharge apparatus. The –OH group-linked resins were heated with TES adsorbed on the resin surfaces, and TES was chemically linked to the resin surfaces to yield TES-linked resins. We heated TES-linked resins with halogen-containing rubber compounds to obtain resin/rubber adherends. Peel strength was influenced by the TES treatment conditions, namely, TES concentration in an ethanol solution and reaction temperatures between the adsorbed TES and the –OH groups on the resin surfaces. The concentration and reactivity of curing agents as well as rubbers had an effect on peel strength. Many resins, except for PP, adhered to rubbers during curing. The results indicated a low material dependence of resins for adhesion. The low adhesion properties for PP were due to the low –OH group concentration, which was obtained by the corona discharge treatment. The linked TES concentration dominated peel strength, rubber coverage, and failure behavior in the peeling test.

In the molecular adhesion technique, it is extremely important that functional groups, which react at interfaces during the adhesion of materials, are present on the surfaces to reduce the material dependence. To introduce functional groups onto many material surfaces, –OH groups must first be present. Metals and ceramics inherently have –OH groups on their surfaces. Using atmosphere corona discharge treatment, it is possible to add –OH groups to the surfaces of organic materials such as resins and vulcanizates[1,2] . The –OH groups widely react with alcoxysilyl groups to yield ether linkages[3] (Fig. 1). Fig. 2 shows C1s components in the XPS analyses of nylon 6 (PA6) surfaces before and after corona discharge treatment. On the PA6 surfaces before corona discharge treatment, C1s peaks assigned to $=CH_2$, C=O, and C–NH groups appeared. Further, after corona discharge treatment, C1s peaks assigned to new –OH and –COOH groups appeared. Fig. 3 shows the effects of 1,3,5-triazine-2,4,6-trithiol (TT), concentration and torque on peel strength of adherents between ECOG and PA6 resin using the molecular adhesive TES. Here, the TES concentration and the linked TES concentration were always constant. We estimated that the interfacial bond concentration remained constant regardless of the TT concentration. Peel strength decreased with an increase in the TT concentration and torque.

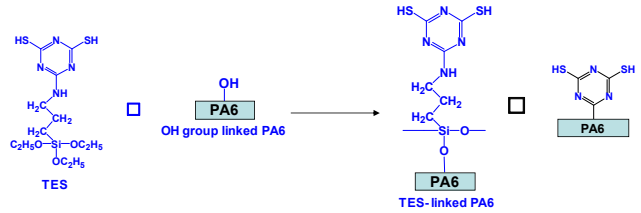

Fig. 1. **Reaction of OH-linked PA6 with TES**

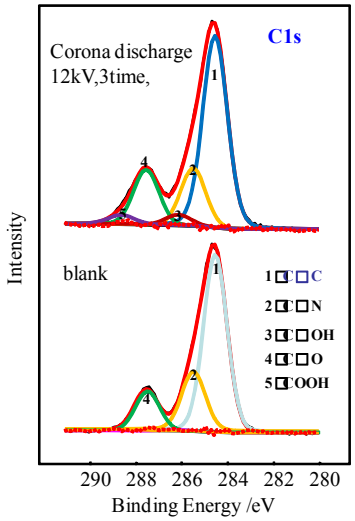

Fig. 2. **C1s components in the XPS analysis of resin surfaces before and after corona discharge**

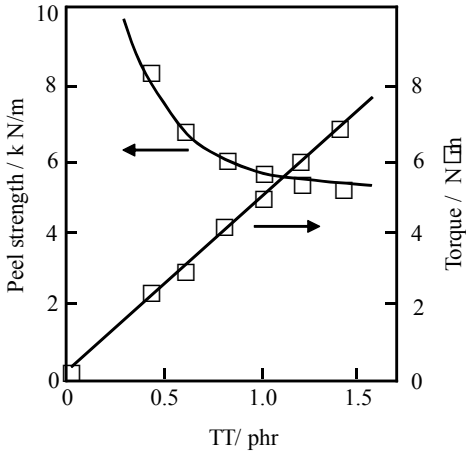

Fig. 3. **The effects of TT concentration and torque on peel strength of adherents between ECOG and PA6 resin using the molecular adhesive TES. Curing conditions: 160 °C × 20 min, 10 MPa**

The increase in the TT concentration and torque brought an increase in the modulus of ECOG vulcanizates. The increase of the modulus decreased peel strength in a 90° peeling test for two reasons. One was a decrease in the tearing strength of ECOG vulcanizates[12,13] and the other was a decrease in the interfacial area between ECOG and PA6 on which stress was applied during the peel testing. Fig. 3 the effects of TT concentration and torque on peel strength of adherents between ECOG and PA6 resin using the molecular adhesive TES. Curing conditions: 160 °C × 20 min, 10 MPa.

We investigated the effects of TES concentration on peel strength in the adherends between ECOG and PA6 resin using the molecular adhesive TES and on the linked-TES concentration ($C_{L\text{-}TES}$) of the PA-6 surface as shown in Fig. 4. TES concentrations in TES ethanol solutions most likely affected peel strengths and the related interfacial bond concentrations. Peel strength increased with an increase in the TES concentration and then reached a plateau. $C_{L\text{-}TES}$ values increased with an increase in the TES concentration and then reached a plateau. The two results indicated a relationship among peel strength, TES concentration, and $C_{L\text{-}TES}$ values. The relationship suggested that peel strength was exhibited by interfacial bonds, which increased with the TES concentration. The TES concentration at both plateaus was different from peel strength and $C_{L\text{-}TES}$. The former was an issue related to interfacial strength and ECOG strength. Fig. 5 shows the failure patterns and types in the peeling test of ECOG and TES-linked PA6 adherends. When the $C_{L\text{-}TES}$ value was zero, we only observed interfacial failure (see Fig. 5(1)) in the peeling test because no interfacial bonds formed in the molecular adhesion technique. In this case, we did observe even small pieces of cured ECOG on the PA6 surfaces because the Ra on the PA6 surfaces after the peeling test was in the range of 40 to 50 nm (38 nm before adhesion). When $C_{L\text{-}TES}$ was in the range of 0.003 to 0.012, small pieces of cured ECOG on PA6

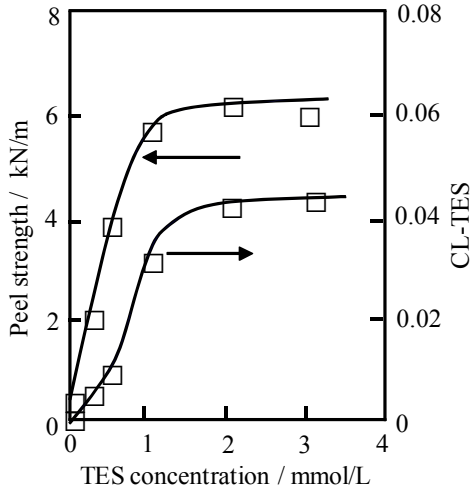

Fig. 4. **Effect of TES concentration on peel strength of adherends between ECOG and PA6 resin using the molecular adhesive TES and on the linked-TES concentration (CL-TES) of the PA-6 surface Corona discharge:** 10.6 kV (59 W), 3.3 mm/s, 2 mm gap. TES treatment: 0–3 mmol/L alcohol solution. 20 °C × 10 min dipping time, 120 °C × 10 min heating. Curing conditions: 160 °C × 20 min, 10 MPa

surfaces were invisible to the eye. However, Ra on the PA6 surfaces after the peeling test increased in the range of 0.1 to 5 μm, meaning that the presence of small pieces of cured ECOG on PA6 surfaces indicated the practical cohesive failure of cured ECOG although it appeared similar to interfacial failure (see Fig. 5(2)). In this case, the failure occurred on the ECOG side because the failure energy of ECOG is considerably smaller than that of PA6. When $C_{L\text{-}TES}$ increased to the range of 0.013 to 0.028, the pieces of cured ECOG on the PA6 surfaces were visible to the eye. We observed peeling surfaces as sea island patterns (see Fig. 5(3)), which consisted of both cohesive and apparent interfacial failures.

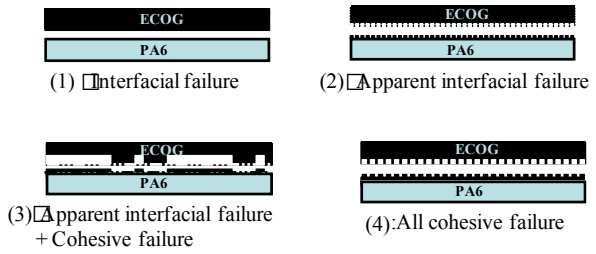

Fig. 5. **Failure patterns and types in the peeling test of CHR and TES-linked PA6 adherends**

REFERENCES
1. Mitsuya T.: Sei Denki Gakkaishi *13*, 17 (1993).
2. Ogawa T.: Nippon Secchaku Gakkaishi *36*, 126 (2000).
3. Nakamura Y., Nagata K.: Sci. Technol., Tokyo (2006).
4. van Ooij W. J.: Rubber Chem. Technol. *51*, 52 (1978).
5. Gent A. N., Kinlok A. J.: J. Polym. Sci., A-2, 9, 659 (1971).

P-14
THERMAL STABILITY OF MODIFIED NANOCOMPOSITE PP FIBERS FOR SILICATE COMPOSITES

ĽUBA HORBANOVÁ[a], JANA VNENČÁKOVÁ[b], ANNA UJHELYIOVÁ[a], and JOZEF RYBA[a]

[a]Department of Fibers and Textile Chemistry, Institute of Polymer Materials, Faculty of Chemical and Foot Technology, Slovak University of Technology in Bratislava, Radlinského 9, 812 37 Bratislava, [b]Research Institute for Man-Made Fibers, a.s., Štúrova 2, 059 21 Svit, Slovakia
luba.horbanova@stuba.sk

Introduction

Fiber reinforced concrete is in the present firmly established as worldwide most commonly used construction material. The term fiber-reinforced concrete is defined as concrete containing dispersed randomly oriented fibers[1−3]. The 3D reinforcement of the concrete results in post-elastic property changes that range from subtle to substantial, depending upon a number of factors, including matrix strength, fiber type, fiber aspect ratio, fiber strength, fiber surface bonding characteristics, fiber content, fiber orientation, aggregate size effects, and the like[4].

Practical function of fibers is to protect composite against sudden failure at the crack initiation in matrix. The tension is transferred to the fibers until the ultimate strength of fibers is reached[5,6]. The enhanced properties include also tensile strength, compressive strength, elastic modulus, crack resistance, crack control, durability, fatigue life, resistance to impact and abrasion, shrinkage, expansion, thermal characteristics, and fire resistance[4].

The basic kinds of large-tonnage fiber-forming polymers and the fibers made from them include polypropylene (PP) and PP fibers. PP fibers are used as reinforcement in construction applications for many years. There is a wide variety of applications of PP fibers in concrete including general constructions and specifically in ground-floor slabs. PP fibers are easy and inexpensive to prepare, easy to disperse and confer advantageous reinforcing properties to the composite materials[7,8].

However, PP fibers also have their specific features which do not always allow arriving at the optimum consumer properties for the fiber materials and articles made from them[7]. This insufficiency is possible to eliminate with fiber modification. More intense anchoring of polypropylene fibers in cement matrix is reached by physical and chemical modification. Addition of sufficient additive ensures that fibers are consistently fixed in matrix. This leads to expressive improve of functional of PP fibers in relation to transmission and absorption of deformation energy to form and load silica composites.

By the addition of additives the structure of polypropylene fibers and by this the properties of fibers may be changed. In this work the thermomechanical and mechanical properties of standard PP fibers and PP fibers modified by inorganic additives with content 2 wt.% and 4 wt.%, before and after stabilization were studied. Information about fiber structure was obtained from TMA scans showing shrinkage behavior before melting. The extent of shrinkage and the temperature at which shrinkage takes place depend on the orientation and crystallinity of the samples[9].

Mechanical properties of fibers were study by investigation of characteristics as tenacity at the break, Young's module and elongation of PP fibers with and without stabilization.

Experimental

Material used

In this study polypropylene (PP) TATREN HT 1810 with MFI = 20.9 g min^{-1} produced by Slovnaft a.s., Bratislava (SK) was used for the preparation of concentrates and fibers modified by inorganic additives. The PP with different content of inorganic additive has been mechanically mixed and melted using the two screw extruder. The obtained PP/ nanoadditive concentrates have been used at the preparation of PP composite fibers by continual technology. PP fibers were used in a form of standard fiber (PP/S) and composite PP fibers. Content of inorganic additive in composite PP fi-

bers was 2 wt.% (PP/C2) or 4 wt.% (PP/C4).

PP/S and PP/C fibers were drawn on the different draw ratios (λ) in the range 2.0–4.0. Samples were exposed the stabilization. Stabilization of PP fibers was carried out at 95 °C for 1 minute.

Methods used

Thermomechanical properties of PP/S and PP/C fibers were performed using Shimadzu Thermomechanical Analyzer TMA-50. TMA dependences were used for determine temperature (T_D) at which the fiber is deformed as well as total deformation – shrinkage (l_D) of fiber at 90 °C. Measurement were carried out at following conditions: heat from room temperature to 90 °C at the heating rate 5 °C min^{-1}, and fiber length 9.8 mm.

Mechanical properties (tenacity at the break, Young's modulus, elongation) were measured by Instron 3343 device and evaluated using Instron program. Tensile test was done in order to measure the tension of fiber to tensile stress until the interruption of fiber. Fibers are straining continuously. Maximum tensile tenacity at the break and corresponding extension is measured at the rupture of fiber. Measuring conditions were the length of fiber 125 mm and rate of clamp 500 mm min^{-1}.

Results and discussion

Thermomechanical properties of PP/S and PP/C fibers with drawing ratio of 2.0–4.0 were evaluated by TMA. Dimensional stability was measured in dependence on temperature growth from room temperature to 90 °C at rate 5 °C min^{-1}. Shrinkage temperatures and total shrinkages of PP fibers with and without stabilization at 90 °C were obtained from experimental dependencies. The results are shown in Tabs. I and II.

From obtained results it is obvious that shrinkage takes place at all measured PP fibers. At both, stabilized PP fibers and PP fibers without stabilization the values of shrinkage were measured higher after addition of inorganic additives. However, increase of content of inorganic additives in PP fibers to 4 wt.% does not lead to growth of shrinkage, but obviously, the shrinkages decrease. The increase of draw ratio of fibers causes decrease of shrinkage.

These results are confirmed by values of temperature at which the fiber deforms. After stabilization the values of deformation temperatures of fibers with addition of inorganic additives are more comparable to standard fibers. At higher draw ratio the influence of modification with inorganic additives on dimensional stability of PP fibers decreases.

In this part mechanical properties of standard and composite PP fibers were evaluated. Tenacity at the brake (σ), Young's module (E) and elongation (ε) of standard and composite PP fibers were measured without and after stabilization (at 95 °C for 1 min, Figs. 1, 2 and Tab. III).

Tenacity at the break and elongation of composite PP fibers without stabilization are decreasing with rising content of inorganic additives and in compare to standard fiber. At higher draw ratio values of tenacity at the break are growing while elongation decreases. After the stabilization tenacity at the break and elongation were found to be comparable to fibers without stabilization.

Table I
Temperature (T_D) of standard PP fibers and composite PP fibers with 2 wt.% and 4 wt.% content of inorganic additives without stabilization (ws) and after stabilization (as)

	T_D[°C]					
λ	PP/S ws	PP/C2 ws	PP/C4 ws	PP/S as	PP/C2 as	PP/C4 as
2.0	52.4	47.1	48.3	50.4	49.7	48.8
2.5	55.5	50.9	49.6	50.8	49.0	51.5
3.0	54.9	50.4	55.4	53.0	52.9	52.1
3.5	56.8	51.3	57.2	55.7	54.3	56.0
4.0	57.4	57.2	54.6	54.5	54.2	54.3

Table II
Shrinkage (l_D) of standard PP fibers and composite PP fibers with 2 wt.% and 4 wt.% content of inorganic additives without stabilization (ws) and after stabilization (as)

	l_D[%]					
λ	PP/S ws	PP/C2 ws	PP/C4 ws	PP/S as	PP/C2 as	PP/C4 as
2.0	–6,5	–12,2	–9,5	–6.5	–10,6	–10.7
2.5	–5,9	–11,1	–8,4	–6.9	–10,0	–7.9
3.0	–6,0	–9,9	–7,6	–7.4	–9,1	–7.4
3.5	–4,1	–6,7	–4,2	–3.8	–4,3	–4.3
4.0	–3,7	–3,7	–5,7	–4.1	–6,0	–5.7

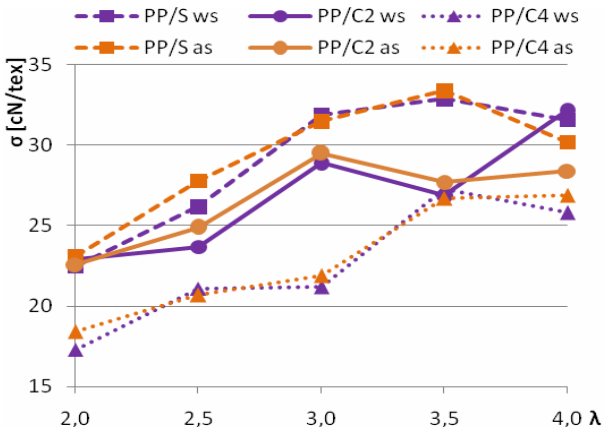

Fig. 1. **Tenacity at the break (σ) of standard and composite PP fibers with different concentration of inorganic additives stabilized at 95 °C during 1 minute (as) and without stabilization (ws)**

By measuring Young's module it was detected, that attributes of standard and composites fibers are comparable and growing with increasing of draw ratio. After the stabilization was at standard PP fibers detected lower Young's module

Table III
Elongation (ε) of standard and composite PP fibers with different concentration of inorganic fillers without stabilization (ws) and after stabilization (as)

	ε [%]					
λ	PP/S ws	PP/C2 ws	PP/C4 ws	PP/S as	PP/C2 as	PP/C4 as
2.0	191	187	168	203	187	172
2.5	144	134	127	154	135	129
3.0	112	105	106	113	99	107
3.5	97	86	75	95	82	74
4.0	74	81	82	74	72	85

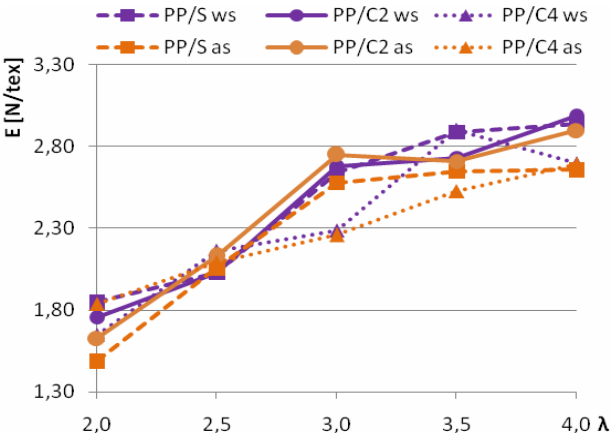

Fig. 2. **Young's module (E) of standard and composite PP fibers with different concentration of inorganic additives stabilized at 95 °C during 1 minute (as) and without stabilization (ws)**

than at samples without stabilization. By addition of inorganic additives are values of Young's modulus approaching to samples without stabilization.

Conclusions

This work was aimed on evaluation of thermomechanical and mechanical properties of standard and composite PP fibers drawn on the different draw ratio. Measurements were realized without and after stabilization of PP fibers.

Thermal stability of PP fibers with addition of inorganic additives was achieved higher at PP/C4 fibers with draw ratio 3.5.

Also at measurements of mechanical properties higher tenacity at the break and Young's module was found at higher draw ratio of PP standard and composite fibers. However, elongation with growth of values of draw ratio decreases.

This work was supported by the Slovak Research and Development Agency under the contract VMSP-P-0007-09 and VEGA 1/0444/09.

REFERENCES

1. Sideris K. K., et al.: Construction and Building Materials *23*, 1232 (2009).
2. Zollo R. F.: Cem. Concr. Compositer *19*, 107 (1997).
3. Banfill P. F. G.: Cem. Concr. Composites *28*, 773 (2006).
4. Trottier J. F., Mahoney M.: Fiber reinforced building materials, US Patent No.: 6,423,134, (2002).
5. Noumowe A.: Cem. Concr. Res. *35*, 2192 (2005).
6. Singh, S., et al: Cem. Concr. Res. *34*, 1919 (2004).
7. Perepelkin K. E.: Fibre Chem. *37*, 2 (2005).
8. Hansen A. S.: Patent number 5,330,827; Date of patent 19.jul 1994.
9. Chand S., Bhat G. S., Spruiell J. E., Malkan S.: Thermomechanical Acta *367-368*, 155 (2001).

P-15
ELECTRON MICROSCOPE, MORPHOLOGY AND STRUCTURE DETERMINATION OF POLYMERS BY CONFINED THIN FILM TECHNIQUES

MARTINA HŘIBOVA and FRANTIŠEK RYBNIKÁŘ*

Tomas Bata University in Zlin, Department of Production Engineering, Czech Republic
rybnikar@ft.utb.cz

Abstract

Advantages of the confined thin film polymerization and crystallization technique are shown on some examples of various polymers. The method requires only a very small amount of sample for crystallization, orientation and additional transformation studies. The effects of various substrate modifications on the polymer structure and morphology are illustrated.

Introduction

Besides crosslinked and very high molecular weight materials stiff and high crystalline aromatic polyesters and polyamides belong to this group also. A big problem, however, is the study of the detailed morphology and crystal structure of such intractable materials by electron microscopy and electron diffraction. These methods demand samples of a suitable thickness and orientation which are not easily attained, e.g., by ultrasectioning. For this reason we have developed a special technique which is based on simultaneous monomer polymerization and crystallization in a confined thin narrow space between two flat solid surfaces (CFTP) resulting in a polymer sample of suitable thickness, structure and orientation[2]. The CTFP method could be used for polymers normally prepared by melt, solution or gas phase polymerization. The aim of this article is to show some typical examples which illustrate the advantage of using the CTFP method.

Experimental

Substrates: As substrates, mostly flat, clean or surface modified glass cover slips or freshly cleaved mica (muscovite) sheets were used.
Samples: For illustration, mainly the laboratory prepared samples of aromatic polyesters and polyamides such as poly-*p*-oxybenzoate (pOB), poly-2,6-oxynaphtoate (pON) and poly-*p*-benzamide (pBA) were used.

Results and discussion

The CTFP technique is a simple, versatile and low cost method accessible in every laboratory with many advantages for polymer research:

1. Sample thickness.
The main advantage is an easy preparation of samples ideally suited for EM and ED examination with a minimum amount of polymer material. The sample thickness can be adapted by the amount of monomer used: a few drops of 0,1−0,5 % monomer solution in a suitable solvent (acetone e.g.).

2. Polymerization mechanism and rate.
We have established with aromatic polyesters and polyamides that in CTFP the polycondensation reaction proceeds much faster than in bulk melt or solution polymerization due to the catalytic effect of the large solid surface[1].

3. Sample crystallization and orientation.
Due to capillary and surface adhesion forces in the closely spaced solid surfaces the polymer tends to polymerize and crystallize in a highly regular conformation e.g. monolayered single crystals or their multilamellar aggregates with a regular crystallographic orientation[3,4].

4. Epitaxial crystallization.
Many crystalline polymers tend to epitaxial crystallization on crystal surfaces of other compounds[5]. In CTFP this tendency is even enhanced. The epitaxial overgrowth is highly crystalline and preferentially oriented in some principal crystallographic directions. Example of P-4-OB and PONA are shown in Figs. 1c,d.

5. Effects of substrate modifications.
For selecting a suitable solid substrate many possibilities are available. Basically, one can select either an amorphous (glass) or crystalline (mica, silica, NaCl), an inorganic or organic, low molecular or high molecular weight substrate. With a given substrate there still are additional possibilities. The substrate can be modified physically or chemically.

Conclusions

The CTFP technique proved useful in the research in a broad range of structure and morphology characterization of various tractable and intractable polymers.

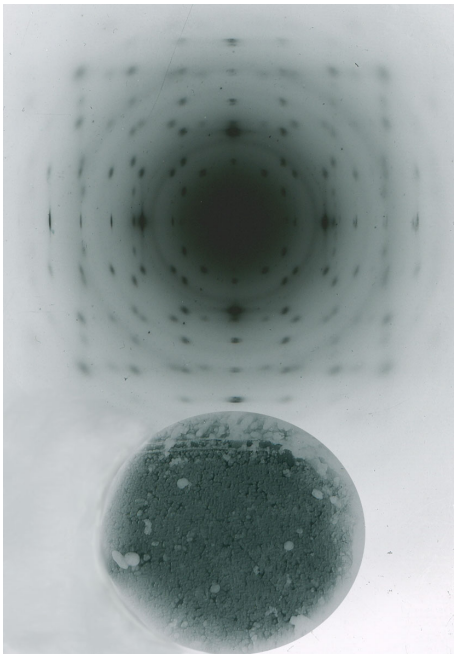

Fig. 1a. **Electron diffraction pattern of POB epitaxially crystallized between mica sheets. Insert is EM bright field of the same sample area**

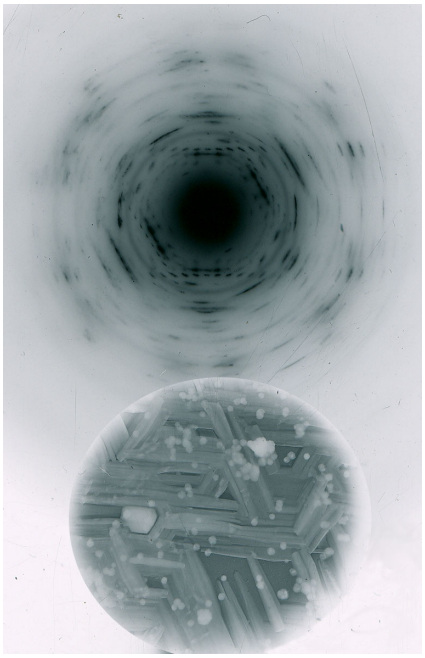

Fig. 1b. **Electron diffraction pattern of PON epitaxially crystallized between mica sheets. Insert is EM bright field of the same sample area**

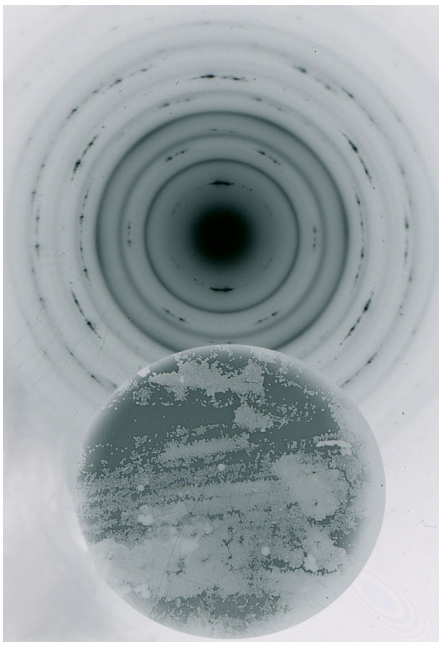

Fig. 1c. **Electron diffraction pattern of PBA epitaxially crystallized between mica sheets. Insert is EM bright field of the same sample area**

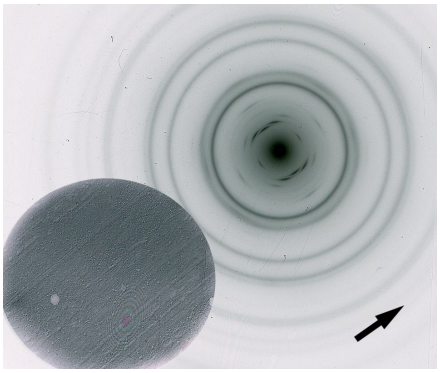

Fig. 2. **Oriented electron diffraction pattern of polyterephthanhydride prepared by shearing monomer polyterephthaloychloride at 200 °C. Arrow indicates the deformation direction**

REFERENCES

1. Liu J., et al. : Polymer 38, vol. 24, 6031 (1997).
2. Rybnikar F., et al. : J. Polymer Sci. Pol. Phys. *37*, 3520 (1999).
3. Rybnikar F., et al. : Macromol. Chem. Phys. *195*, 81 (1994).
4. Rybnikar F., et al.: Polymer *35*, 183 (1994).
5. Wang J., et al.: Macromolecules *29*, 8271 (1996).
6. Manas, M. et al.: Chem. Listy *103*, (2009).
7. Stanek, M. et al.: Chem. Listy *103*, (2009).
8. Manas D. et al. : Chem. Listy *103*, (2009).

P-16
RHEOLOGICAL PROPERTIES OF POLYPROPYLENE COMPOSITES

MARCELA HRICOVÁ[a], ĽUBA HORBANOVÁ[a], ANTON MARCINČIN[a], ŠTEFAN KRIVOŠ[b], and ANNA UJHELYIOVÁ[a]

[a] Slovak University of Technology in Bratislava, FCHFT, IPM, Department of Fibres and Textile Chemistry, Radlinského 9, 812 37 Bratislava, [b] Research Institute for Man-Made Fibers, a.s., Štúrova 2, 059 21 Svit, Slovak Republic
marcela.hricova@stuba.sk

Polypropylene fibres are often used as a reinforcing material in construction applications. Special polypropylene fibres show poor adhesion with cement matrix due to their hydrophobic character and smooth surfaces[1]. Desired fixation of PP fibres in cement matrix can be achieved by physical and chemical modification of PP. Addition of suitable additive insures that fibres are consistently fixed in matrix.
Fibers as a reinforcing material in cement matrix can improve both tension and compression mechanical resistance, improve impact resistance, control cracking and kind of fracture by means of improved ductility after cracking as well as modify rheology and material flow[2].

The effect of the silica and selected organic additives as dispersants on the rheological properties of polypropylene (PP) composite melt is discussed in this paper. Rheological parameters such as apparent viscosity and deviation from the Newtonian flow, expressed by exponent of the Oswald-de Vaele equation, as well as activation energy of melt flow were used for estimation of the melt processing of the PP/SiO_2 composites at melt spinning and preparation of the PP composite fibres used as fibrous filler for construction of composites with inorganic e.g. cement concrete matrix.

The mixture of inorganic additives and PP was processed using twin-screw extrude (Φ 28 mm). The composites containing 8 or 10 wt.% of inorganic additives (S) and 2 wt.% of dispersants (A, B, C, D, E and F) were prepared.

The rheological properties of the PP composites were measured using a capillary extrusiometer Göttfert N 6967 (ϕ = 20 mm).

The viscosity of PP composites increases with content of additives and decreases with temperature. Deviation from the Newtonian behaviour, expressed by power law exponent n, is the highest for pure polypropylene. In addition, the melt viscosity for PP is the lowest. The presence of silica solid particles in PP composites decreases the deviation from Newtonian behaviour but at the same time increases the melt viscosity (Table I). The values of melt viscosity are very similar for PP/S composites regardless of type of used dispersants.

The dispersants A, B and C show slightly positive effect on melt viscosity of PP/S composites, mainly at higher temperatures and lower shear rate. The higher values of power law exponent of PP/S composites with dispersants reveal the decrease of the melt elasticity and give an assumption of improved processability of these polymer materials at fibres preparation.

Table I
Power law exponent n and viscosity η of the PP/S composites

PP/S composites	T [°C]	n	η [Pa.s]		
			γ=300 s^{-1}	γ=500 s^{-1}	γ=1000 s^{-1}
PP	240°C	0.38	185	135	87
	260°C	0.44	147	111	76
	280°C	0.46	129	97	66
PP + 8% S + A	240°C	0.45	197	148	101
	260°C	0.49	165	127	89
	280°C	0.54	140	110	80
PP + 8% S + B	240°C	0.42	202	150	100
	260°C	0.47	168	128	88
	280°C	0.53	139	109	79
PP + 8% S + C	240°C	0.43	198	148	99
	260°C	0.47	166	127	88
	280°C	0.51	139	109	77
PP + 8% S + D	240°C	0.43	207	155	104
	260°C	0.47	174	133	92
	280°C	0.51	146	114	82
PP + 10% S + E	240°C	0.42	225	168	112
	260°C	0.45	194	147	101
	280°C	0.47	169	129	89
PP + 10% S + F	240°C	0.39	208	152	100
	260°C	0.43	177	132	89
	280°C	0.46	151	115	79

Table II
Activation energy of polymer melt flow at assigned shear rate γ

PP/S composites	ΔE [kJ/mol]		
	γ=300 s^{-1}	γ=500 s^{-1}	γ=1000 s^{-1}
PP	21.4	19.2	16.1
PP + 8 % S + A	20.2	17.5	13.9
PP + 8 % S + B	22.3	18.9	14.2
PP + 8 % S + C	20.7	18.2	14.7
PP + 8 % S + D	20.5	17.9	14.2
PP + 10 % S + E	16.8	15.4	13.6
PP + 10 % S + F	18.8	16.6	13.7

Additives and dispersants decrease the activation energy of melt flow of PP/S composites in temperature range 240–280 °C (Table II). It means that the presence of solid particles in PP composites has a positive effect on activate transitions of "independent" segments of polymer chains and facilitate flow of composite melt at spinning.

This work was supported by the Slovak Research and Development Agency under contract No. VMSP-P-0007-09 and VEGA agency No. 1/0444/09.

REFERENCES

1. Lee S. D., Sarmadi M., Denes E., Shohet J. L.: Plasmas Polym. *2*, 177 (1997).
2. Hannant D. J. :*Fibre cement and fibre concrete*, 1st ed. John Wiley & Sons, 1978.

P-17
OPTICAL AND ATOMIC FORCE MICROSCOPY ON FILLED RUBBER COMPOUNDS

SYBILL ILISCH, HAI HONG LE, KATRIN REINCKE, and HANS-JOACHIM RADUSCH

Martin Luther University Halle-Wittenberg, Center of Engineering Sciences D-06099 Halle (Saale), Germany
sybill.ilisch@iw.uni-halle.de

Introduction

The quality of rubber mixtures is strongly dependent on the effective dispersion and uniform distribution of the filler throughout the polymer matrix. Therefore different test procedures have been developed for the characterization of filler dispersion. Microscopical methods on different length scales are an indispensable tool for the characterization of filler dispersion, phase selective filler distribution and phase morphology.

From the beginning of rubber processing, the compounder has used some procedures to determine the quality of mixing. Especially surface inspection of stretched or cutted samples was utilized. In 1956 Leigh-Dugmore[1] quantified the optical microscope analytical procedure to determine the percentage of carbon black dispersed below a certain agglomerate size (6 μm). His method was adopted by ASTM and is still widely used today (Dispersion Index). Stumpe and Railsback[2] used photographic technique in connection with a rating system for the characterization of the carbon black dispersion (Dispersion Degree).

After the invention of the atomic force microscope (AFM) this technique was also applied for the investigation of filled rubber blends [3–9].

Experimental

Optical Microscopy

The comparison between estimated dispersion index and dispersion degree as measure of the filler macro dispersion was conducted for industrial mixed samples (75/25 NR/E-SBR blend with 50 phr N 330, Banbury Pomini 3.5 l, fill factor 0.7, n=80 rpm, T_A=70 °C, T_D= 140 °C). The values show a similar trend: with increasing mixing time the dispersion index and the dispersion degree increase (Fig. 1).

For the calculation of dispersion index gloss cuts were produced by cutting thin, stretched samples by a razor blade at room temperature. If the surface of the cut contents filler agglomerates or aggregates, the light is scattered and its area

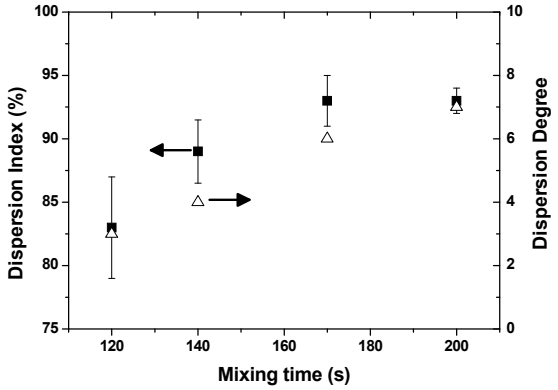

Fig. 1. **Dispersion index and dispersion degree versus mixing time for CB filled NR/SBR blend**

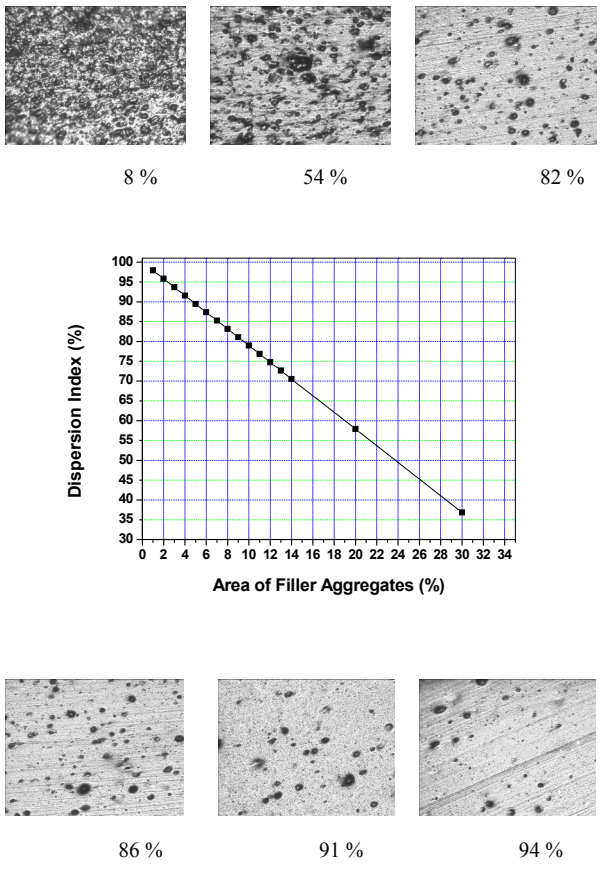

Fig. 2. **Dispersion index versus area of filler aggregates and optical micrographs for different dispersion states**

appears dark. With a Leica image analysis program the area of larger filler regions was calculated (Fig. 2). The dispersion degree was assessed as the amount of the non-dispersed agglomerates with an average diameter larger than 6 μm. After processing microscopic visualization image analysis was used to quantify the degree of filler dispersion. A dispersion index of 100 % means that no aggregate size larger than 6 μm could be found in the cut surface. From each sample 6 pictures were made and from each picture 6 image analyses were taken.

$$D = (1 - \frac{\frac{1}{n}\sum_{i}^{n}(A \cdot \phi_{Med})}{\phi \cdot A_0}) \cdot 100\ \% \qquad (1)$$

The macro dispersion index D (Eq. *1*)[10] is assumed to be the ratio of the sum of the surfaces, which can be assigned to non-dispersed filler clusters and exhibit a diameter larger than 6 μm (A) with respect to the whole viewed surface (A_0). φ is the volume fraction of the filler and φ_{MED} the Medalia[11] factor, which is linked with the effective volume of the filler, in case of carbon black 0.4.

Atomic Force Microscopy

For the creation of AFM phase images a very smooth sample surface is essential. We cut the samples in frozen state in a cryo-chamber by diamond knife in microtom. Fig. 3 shows the filler dispersion for 75/25 NR/E-SBR blends with 50 phr N 330 mixed in Banbury Pomini 270 l, n=40 rpm, T_A=120 °C, T_D= 165 °C, t=190 s for variable fill factors (Table I).

Table I and Fig. 3 show the correlation between macro and micro dispersion: with increasing macro dispersion also the micro dispersion of filler increases. The bright areas in the

Table I
Sample names, fill factors and dispersion index

Sample	F1	F3	F5
Fill Factor	0.64	0.70	0.775
Dispersion Index, %	94.2 +/– 2.3	95.4 +/– 2.1	97.6 +/– 0.9

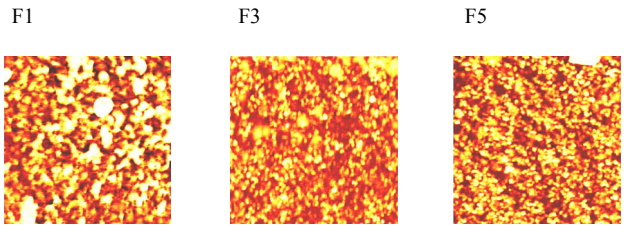

Fig. 3. **AFM images (5 × 5 μm), made in intermittend mode on diamond knife cutted samples (–100 °C) according Table I**

Table II
Results of dimensional analysis of different carbon black types in an E-SBR matrix (50 phr CB, Brabender Plasticorder N 50, n=50 rpm, T_A=50 °C, T_D= 85 °C, t=20 min, fill factor

Carbon Black	N 220	N 330	N 550	N 772	N 990
Particle Size, nm	20-25	26-30	40-48	61-100	201-500
Size of largest Aggregate, nm	440	510	725	572	827
Size of smallest Aggregate, nm	290	220	128	151	186

shown pictures are filler aggregates, the darker areas rubber regions of different hardness.

The quantitative dimensional analysis of CB aggregates of different CB types shows an increasing number of particles included in the aggregates with decreasing dimension of CB primary particles (Table II).

Recently a correlation between the fracture surface roughness and the toughness[12] could be shown (Fig. 4).

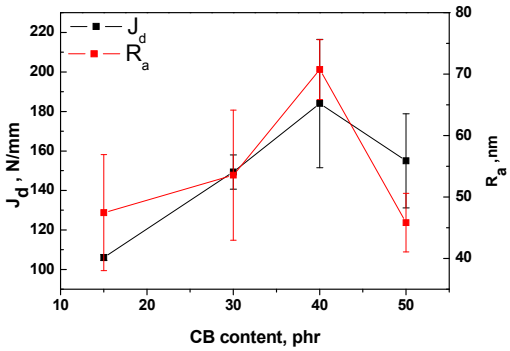

Fig. 4. **Fracture toughness J_d and roughness R_a versus carbon black content (E-SBR, N330)**

Conclusions

Optical microscopy and AFM are suitable tools for the visualization and quantification of filler dispersion in the scale of 500 μm to 50 nm. AFM images can also be used to show the roughness of sample surfaces. In case of blends with high filler content similar dimensions of filler aggregates and polymer phases hinder the quantification of filler localization in different blend phases.

The authors thank the German Research Foundation (DFG) for the financial support of this work.

REFERENCES

1. Leigh-Dugmore C. H.: Rubber Chem. Technol. *29*, 1303 (1956).
2. Stumpe N. A. Jr., Railsback H. E.: Rubber World *151*, 41 (1964).
3. Galuska A. A., Poulter R. R., Mc Elrath K.O.: Surf. Interface Anal. *25*, 418 *(*1997).
4. Ganter M., Brandsch R., Thomann Y., Malner T., Bar G.: KGK, Kautsch. Gummi Kunstst. *52*, 717 (1999).
5. Herrmann V., Unseld K., Fuchs H. B.: KGK, Kautsch. Gummi Kunstst. *54*, 453 *(*2001).
6. Jeon I. H., Kim H., Kim S. G.: Rubber Chem. Technol. *76*, 1 *(*2003).
7. Wang C. C., Donnet J. B., Wang T. K.: Rubber Chem. Technol. *78*, 17 (2005).
8. Bielinski D.M.: Kautsch. Gummi Kunstst. *58*, 239 (2005).
9. Johnson L. L.: Rubber Chem. Technol. *81*, 359 (2008).
10. Radusch H.-J., Androsch R., Ilisch S.: Practical Metallography *48*, 29 (2011).
11. Boonstra B. B., Medalia A. I.: Rubber Chem. Technol. *36*, 115 (1963).
12. Horst T., Reincke K., Ilisch S., Heinrich G., Grellmann W.: Phys. Rev. E80, 046120 (2009).

P-18
PREPARATION AND CHARACTERIZATION OF POLYMER BLENDS OF POLYETHYLENE WITH GALACTOMANNAN-PART II

PETRA SKALKOVÁ[a], ZUZANA JAKUBÍKOVÁ[b], and DANIELA JOCHEC-MOŠKOVÁ[c]

[a] Faculty of Industrial Technologies, Trenčín University of A. Dubček, I. Krasku 491/30, 020 32 Púchov, [b] Vitrum Laugaricio – Joint Glass Center of IIC SAS, TnU AD, FCHPT STU and RONA, j.s.c., Študentská 2, 911 50 Trenčín, [c] Polymer Institute, Slovak Academy of Sciences, Dúbravská cesta 9, 842 36 Bratislava, Slovak Republic
skalkova@fpt.tnuni.sk

Abstract

This work deals with blends preparation low density polyethylene and locust bean gum (LBG) with degree of substitution DS 0,28 in four different amounts (0, 5, 10, 25 wt.%) with and without compatibilizer EAA in three different amounts: 10, 25 and 50 wt.% in respect of polysaccharide. The presence of filler LBG and the effect of compatibilizer have been studied through the mechanical properties (tensile strength, elongation at break and Young`s Modulus) of blends. TGA, DMA and REM were employed to determine the structure and properties of the blends. Increasing amount of LBG and presence of compatibilizer had positive effect on thermal stability of LDPE/LBG blends.

Using of polyolefins and polysaccharides and their relative compatibility

Polyolefins are very important and useful synthetic polymers because they posses good properties, well-known technology of production and low cost. A representative polyolefins used as packaging materials are high density polyethylene (HDPE), low density polyethylene (LDPE) and polypropylene (PP). Since the use of these plastics is continuously increasing, the problem of post-consumer recycling of these materials has become an important issue for economic and environmental reasons[1,2]. An increasing interest in the recycling and the use of biodegradable materials, with the aim of improving thermo-mechanical properties of polymer blends, has lead to the use of polysaccharides as biodegradable filler. The greatest application of polysaccharides, especially starch, cellulose, xylans and their derivatives in the polymers field are as a component in various polymer formulations[3]. Most of the applications are focused on polyethylene, which is widely used as packaging material and in automotive. Polysaccharides are hydrophilic macromolecules, while polyethylene is hydrophobic. The difference in their properties results in poor compatibility of polysaccharide/polyethylene blends. One approach in achieving miscibility and improving adhesion of phases is to replace the hydrophilic OH groups of polysaccharide with hydrophobic groups through esterification. Another way to increase compatibility, and thus the incorporated amount of polysaccharide in polyethylene blends, is to use a compatibilizer containing groups capable of hydrogen bonding with polysaccharide hydroxyls. The most frequently used compatibilizer is ethylene/acrylic acid copolymer (EAA)[4].

Galactomannan specification

Locust bean gum (LBG) is a polysaccharide built up of a main chain of mannose units with short branches of single galactose units. The molecular weight of locust bean gum is 310 000 g mol^{-1}. An average quality locust bean gum contains 12 % moisture, 0,7 to 1,5 % acid insoluble ash, and 6 % protein[6]. Locust bean gum is compatible with other hydrocolloids as well as carbohydrates and proteins. LBG is extremely versatile as thickener or viscosity modifier, binder of free water, suspending agent and stabilizer[5,6].

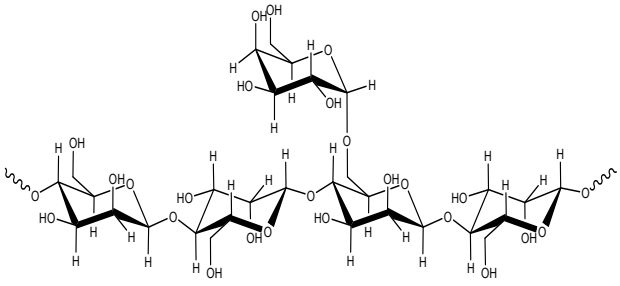

Scheme 1. **Structural unit of locust bean gum**

This work was supported by the Slovak Grant Agency for Science under the grant No. VEGA 1/0330/09 and by the Agency for Promotion Research and Development under the contract No. APVV LPP-1-0156-09.

REFERENCES

1. Pracella M., Pazzagli F., Galeski A.: Polymer Bulletin, *48*, 67 (2002).
2. Ishiaku U. S., Pang K. W., Lee W. S., Ishak Z. A.: Eur. Polymer J. *38*, 393 (2002).
3. Heyde M.: Polym. Degrad. Stab. *59*, 3 (1998).
4. Willett J. L.: J. Appl. Polym. Sci. *54*, 1685 (1994).
5. Smith J., Hong-Shum L.: *Food Additives data book:* Part X. Polysacharides: Locust Bean Gum, 2003.
6. Wang J., Somasundaran P.: J. Colloid Interface Sci. *309*, 373 (2007).
7. Koštial P., Ružiak I., Jonšta Z., Tvrdý M.: Defect and Diffusion Forum *297*, 30 (2010).

P-19

REMOVAL OF RESORCINOL FROM WATER SOLUTION BY USING M-EXCHANGED MONTMORILLONITE (M = Co, Ni)

RÓBERT JANÍK, EUGEN JÓNA, SOŇA ŠNIRCOVÁ, DARINA ONDRUŠOVÁ, and MARIANA PAJTÁŠOVÁ

Department of Chemical Technologies and Environment, Faculty of Industrial Technologies, University of Trenčín, 020 32 Púchov, Slovakia
janik @fpt.tnuni.sk

Phenol and its derivatives (especially resorcinol) are the priority pollutants since they are toxic and harmful to organism even at low concentrations. Surface and ground waters are contaminated by resorcinol as a result of the release of these compounds from rubber, petrochemical and other phenol producing industries[1].

The immobilization and detoxification of hazardous substances with clay minerals represents a vital area for research. Smectites (especially montmorillonite) have a layered structure and adsorb the organic pollutants and also can catalyze their chemical transformation[2–4]. In this paper x-ray diffraction and infrared absorption spectra have been used to study the removal of resorcinol (3-hydroxy phenol) from water solutions by using Co- and Ni- exchanged montmorillonite. It was found, that resorcinol was successfully intercalated into interlayer spaces of Co- and Ni- exchanged montmorillonite. Resorcinol may form a hydrogen bond with the water molecule and accept a proton from this acid species. The absorption of resorcinol depends on the experimental conditions (the concentration of resorcinol, time of interactions).

REFERENCES

1. Yapar S., Yilmaz. M.: Adsorption *10*, 287 (2004).
2. Yariv S.: Thermochem. Acta *274*, 1 (1996).
3. Ovadyahu D., Yariv S., Lapides I., Deutsch Y.: J. Therm. Anal. *51*, 431 (1998).
4. Šnircová S., Jóna E., Lajdová Ľ., Jorík V., Drábik M., Pajtášová M., Ondrušová D., Mojumdar S. C.: J. Therm. Anal. Cal. *96*, 63 (2009).

P-20
METHODS FOR EVALUATION OF SLOVNAFT′S PETROCHEMICALS IMPACT AND TERMOPLASTIC PP COPOLYMER GRADES PROPERTIES ATTRACTIVE TO THE AUTOMOTIVE INDUSTRY

EVA KAMESCHOVÁ

Slovnaft Petrochemicals, s.r.o., Product and Application Development, Vlčie Hrdlo 4846, 824 12 Bratislava, Slovak Republic
eva.kameschova@petchem.sk

Slovnaft Petrochemicals, s.r.o., the member of MOL Group, is producer of two different polyolefines. LDPE – registered trademark Bralen and PP (homopolymers, ethylene /propylene random and impact (block) copolymers) – registered trademark Tatren.

Impact copolymers (IM) and thermoplastic copolymers (TPO) were tailored for automotive industry demands. IM copolymers, with broad range of MFR (from 6 to 100 g/10 min), have very good balance between the toughness and stiffness and due to these excellent properties have very broad utilization in injection moulding of rigid packaging, storage, medical and transport boxes and containers, household appliances, garden furniture, auto battery cases and other technical items. TPO copolymers are, due to excellent impact properties, suitable for compounding, automotive applications and bumpers.

There is variety of properties which can be determined but each has not equal importance for different usage area. For example as regards automotive industry the most crucial are content of C – emissions, Ethylene Content, impact properties (such as Izod Impact vs. Gardner), Modulus of Elasticity in Flexure (bidirectional), Shrinkage, Demoulding Force and Cycle Time (checked by thermal properties).

C – emissions are evaluated from final pellets by method designed for GC/Static Headspace with Flame Ionization Detector (FID). Exact amount of sample is preheated in glass vials for specific time and temperature. Organic compounds are evaporated from the heated sample and released into the space above pellets. When equilibrium is reached, the concentration of the volatiles in the headspace is at its maximum and it is injected onto the analytical column for separation Then the C – emissions potential is measured on the basis of the sum of all values provided by the emitted substances after gas chromatography analysis and flame ionization detection[1].

Ethylene Content is evaluated by infrared spectroscopy. The point of Ethylene Content evaluation is in monitoring of intensity of recurrented methylene group peak in infrared spectra of samples. We can determine Et (total content of ethylene in copolymer), Ec (content of ethylene in rubber phase) and Fc (content of rubber phase in copolymer) as well.

Impact properties can be measured by Izod Impact or Gardner Impact equipment. Gardner Impact is for American method and it describes the real impact properties better then Izod, because in Izod we use notched samples and hammer is moving from side to side. In case of Gadner Impact weight is falling down onto injection molded sample without notch, so it simulates the real situation for example in car bumpers better[2].

Modulus of Elasticity in Flexure can be interpreted as one-directional or bidirectional mechanical property of material. In the first case sample has rectangular shape and the crosshead is applying the load perpendicular to the flow. In the second case sample has squared shape and crosshead is applying the load perpendicular and parallel to the flow as well. Comparing one-directional and bidirectional testing, the latter announces the isotropy of material in addition to the Flexural Modulus and it fits to the reality better[3].

As regards isotropy of material another very reliable property is Shrinkage. Samples are squared shaped plates prepared by injection molding. Shrinkage is calculated from changing dimensions of plates. First dimensions are determined by dimensions of mold and the second dimensions of plates are measured by calipers after the certain time of conditioning[4].

One option how to influence demoulding of injection molded products is to add appropriate nucleation agents. Reduction of the demoulding time we can measure indirectly through thermal properties determined by Differential Scanning Calorimetry (DSC) such as Temperature of Crystallization (T_c) and Half Time of Crystallization ($t_{1/2}$)[5].

REFERENCES

1. VDA 277, Determination of emission of organic compounds, 1995.
2. ISO 180, Determination of Izod impact strength, 2000 and STN EN ISO 294-1Injection moulding of test specimens of thermoplastic materials, 1996.
3. ISO 179, Determination of flexural properties, 2000.
4. ISO 294 – 4, Injection moulding of test specimens of thermoplastic materials -- Part 4: Determination of moulding shrinkage, 2001.
5. ISO 11357, Differential scanning calorimetry (DSC), 2009.

P-21
INFILTRATION BEHAVIOR OF RUBBER IN SILICA COMPOUNDS

M. KELLER, H. H. LE, S. ILISCH, and H.-J. RADUSCH

Martin Luther University Halle-Wittenberg, Center of Engineering Sciences, D-06099 Halle (Saale), Germany
melanie.keller@iw.uni-halle.de

Abstract

The wetting behavior as pre-step of the infiltration and dispersion of silica by different rubbers during the mixing process in an internal mixer was investigated by extraction experiments and discussed by a new developed model. Compared to the wetting in a stationary state the wetting process in the in-stationary state in internal mixer takes place very fast due to the effect of shear stress and pressure. Addition of silane and curing additives leads to a large change of the wetting behavior of silica.

Introduction

Since the 1990s carbon black is more and more substituted by silica/silan systems as reinforcing filler in rubber compounds for tire applications. The dispersion of filler both silica and carbon black is the key for achieving good quality and consistent product performance of rubber compounds. After incorporation of filler into polymer matrix the polymer molecules start to infiltrate into the pores of the filler agglomerates. The presence of infiltrated polymer within the agglomerate introduce additional forces which have a direct effect on the dispersion ability of filler[1–3]. The rheological behavior of the penetrating polymer is an influencing factor to overcome the cohesive forces of the agglomerates, and consequently on the type of dispersion mechanism rupture or erosion. Astruc et al.[3] recently showed that the more entropy-elastic the matrix, the larger the stress required to erode agglomerates and the slower the erosion proceeds. This was observed in the case where the matrix infiltrated the agglomerates and the more difficult erosion was explained by an increase of the agglomerate cohesiveness due to the elastic character of the penetrated fluid. The knowledge of infiltration kinetics of the polymer inside the filler agglomerate is necessary to understand the dispersion of porous filler during mixing operations. Basis knowledge on the penetration kinetics has been gained in the last decade for CB and silica in Newtonian liquids using a transparent counter-rotating plate-and-plate shear cell coupled with an optical device. Fluid infiltration into agglomerates is driven by capillary pressure, which depends on, amongst other factors, the characteristic pore size and the interfacial tension between fluid and particle surface. Bohin et al.[4] studied the kinetics of the penetration of a Newtonian silicon oil into silica agglomerates in a stationary state. They proposed a model based on the capillary forces driving the penetration and viscous effects resisting it.

In the present work we characterized the infiltration kinetics of rubbers into silica during the real mixing process by means of the rubber-layer *L*, which is determined from the development of the bonded rubber on the silica surface. Effect of rubber viscosity, polarity, and addition of additives as well as mixing conditions on the infiltration process will be discussed by taking into consideration the known theories.

Experimental

The used materials are listed in Table I (ref.[5]). The compounding of the material was carried out in a laboratory internal mixer (Plasticorder PL2000).

To characterize the wetting behaviour of filler by the rubber molecules the rubber-layer *L* was determined by means of the extraction experiment[6] according to eq. (*1*).

$$L = \frac{m_2 - m_1 \cdot c_S}{m_2} \qquad (1)$$

The mass m_1 corresponds to the rubber compound before extraction; it is the sum of the mass of the undissolvable rubber, the mass of the soluble rubber and of silica. m_2 is the mass of the rubber-filler gel, which is the sum of the undissolvable rubber and the mass of silica. c_S is the mass concentration of silica in the mixture.

Table I
Used materials

Name	Trade Name, Supplier	Remarks
BR	Buna® cis 132-Schkopau, Styron Deutschland GmbH	95 % cis-1,4
S-SBR	Sprintan® SLR 4602-Schkopau, Styron Deutschland GmbH	21 % styrene, 63 % vinyl
Silane	NXT Silane, Momentive Performance Materials	3-Octanoylthio-1-propyltriethoxysilane
Silica	Ultrasil 7000 GR, Evonik Europe GmbH	
ZnO	Zinc oxide	
StA	Stearic Acid	
CBS	Vulkacit CZ/EG-C, Rhein Chemie Rheinau GmbH	N-Cyclohexyl-2-benzothiazole sulfenamide
DPG	Vulkacit D/EG-C, Rhein Chemie Rheinau GmbH	Diphenylguanidine

By taking into consideration the eq. 1 the rubber-layer *L* can also be expressed by eq. (*2*):

$$L = \frac{hbt^{1/2}}{hbt^{1/2} + \rho_F(1-\varepsilon)} \qquad (2)$$

The wetting rate *b* is given by eq. (*3*), ref.[7]:

$$b = (2A + 2B)^{1/2} \qquad (3)$$

with $A = \frac{S\gamma_R \cos\theta}{6\eta_R}$; $B = \frac{S^2 \Delta P}{12\eta_R}$ and $S \approx \frac{D_p \varepsilon^2}{2(1-\varepsilon)}$

where *t* is the mixing time, ΔP is the pressure in the internal mixer. D_P, ρ_F and ε are the primary particle diameter, density and porosity of the filler, respectively. γ_R and η_R are the surface tension and viscosity of the rubber, respectively. $cos\theta$ is the contact angle between rubber and filler. The correlation between the plateau value L_P and the factor *h* is described as followed:

$$L_P = \frac{\varepsilon h}{\varepsilon h + \rho_F(1-\varepsilon)} \qquad (4)$$

Results

Wetting of silica by SBR in a stationary state

The infiltration experiment in stationary state was carried out according to the work of Astruct[3]. Two thin films of S-SBR containing a few agglomerates of silica randomly

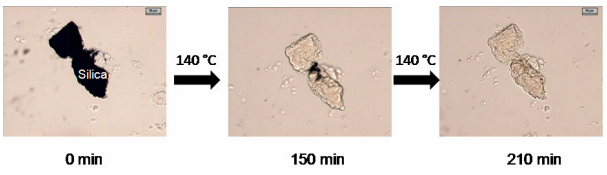

Fig. 1. **Infiltration of silica by S-SBR in a stationary state at 140 °C**

placed in between two glass plates and its thickness is controlled. The infiltration was characterized by optical microscopy by following the change of the dry part of the silica agglomerates vs. time. Non-infiltrated parts of the agglomerates appear black (due to the large difference of refractive index between air and silica), whereas, the infiltrated parts are transparent (small difference of refractive indices between silica and the fluid). It is clear to see from Fig. 1 that a silica agglomerate needs about 150 min to be fully infiltrated.

Effect of additive addition on the wetting behavior at 50 °C

The addition of additives, i.e. ZnO, stearic acid and CBS/DPG, into the S-SBR and the BR mixture obviously elevate the development of *L*. As seen in Fig. 2 additives can fast diffuse into the silica agglomerates thanks its low molecular weight. If the additives get in contact with silica surface, they are able, dependent on type, to interact with silanol groups in various ways. Ramier et al.[8] showed that both CBS and DPG are able to interact with the silica surface whereupon DPG would adsorbed first, because of the stronger basicity. ZnO and stearic acid react via an ion exchange reaction with the silanol groups[9]. The presence of additives on the silica surface changes the filler-filler- and filler-matrix-interaction and thereby the physisorption of rubber molecules to the silica that elevates the formation of the rubber-layer *L*.

Effect of mixing temperature and silane on the wetting behaviour

For BR a significant change of the wetting rate due to mixing temperature or silane is unverifiable as seen in Fig. 3. The calculated wetting rate for all three mixture is b = 0.2.

Conclusions

The wetting behavior of silica by different rubbers during the mixing process in an internal mixer was investigated by extraction experiments and discussed by a new developed model. The Addition of additives leads to a significant change of the wetting behavior of silica. For BR an influence of temperature or silane was not detectable under the chosen conditions.

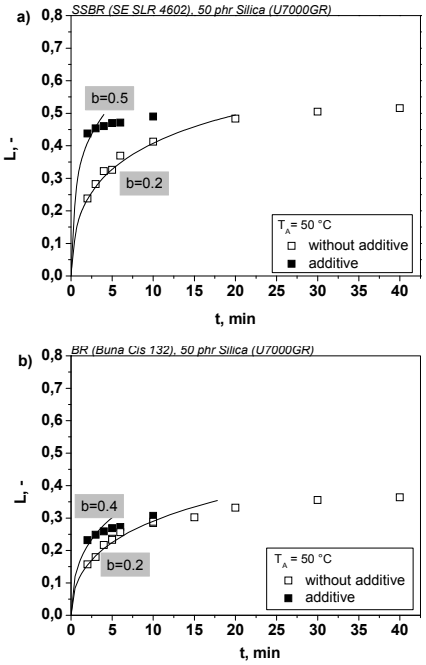

Fig. 2. **Wetting behaviour of silica by S-SBR (a) and BR (b) under influence of additives addition**

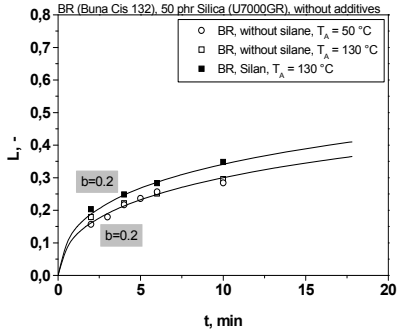

Fig. 3. **Wetting behaviour of silica by BR under influence of temperature and silane**

REFERENCES

1. Levresse P., Feke D. L., Manas-Zloczower I.: Chem. Eng. Sci. *56*, 3211 (2001).
2. Gopalkrishnan P.: *PhD thesis*, Case Western Reserve University Cleveland/USA, 2004.
3. Astruc M., Collin V., Rusch S., Navard P., Peuvrel-Disdier E.: J. Appl. Polym. Sci. *91*, 3292 (2004).
4. Bohin F., Manas-Zloczower I., Feke D. L.: Rubber Chem. Technol. *67*, 602 (1994).
5. Thiele S., Bellgardt D., Holzleg M.: Kautsch. Gummi Kunstst. *5*, 244 (2008).
6. Le H. H., Kasaliwal G., Ilisch S., Radusch H.-J.: Kautsch. Gummi Kunstst. *5*, 241 (2007).
7. Lin C. M., Chang W. J., Fang T. H.: J. Electronic Packaging *129*, 48 (2007).
8. Ramier J., Chauzeau L., Gauthier C.: Rubber Chem. Technol. *80*, 183 (2007).
9. Hewitt N.: *Compounding Precipitated Silica in Elastomers*, William Andrew Publishing, Norwich/USA (2007).